Neural Networks 22 (2009) 890–900

Contents lists available at ScienceDirect

Neural Networks

journal homepage: www.elsevier.com/locate/neunet

Selective attention model with spiking elements

David Chik [a], Roman Borisyuk [a,b,*], Yakov Kazanovich [b]

[a] Centre for Theoretical and Computational Neuroscience, University of Plymouth, Plymouth PL4 8AA, UK

[b] Institute of Mathematical Problems in Biology, Russian Academy of Sciences, Pushchino, Moscow Region, 142290, Russia

ARTICLE INFO

Article history:
Received 3 March 2008
Received in revised form 3 December 2008
Accepted 12 February 2009

Keywords:
Hodgkin–Huxley neurons
Synchronization
Attention model
Sequential selection

ABSTRACT

A new biologically plausible model of visual selective attention is developed based on synaptically coupled Hodgkin–Huxley neurons. The model is designed according to a two-layer architecture of excitatory and inhibitory connections which comprises two central neurons and a population of peripheral neurons. Two types of inhibition from the central neurons are present: fixed inhibition which is responsible for the formation of the attention focus, and short-term plastic inhibition which is responsible for the shift of attention. The regimes of synchronous dynamics associated with the development of the attentional focus are studied. In particular, the regime of partial synchronization between spiking activity of the central and peripheral neurons is interpreted as object selection to the focus of attention. It is shown that peripheral neurons with higher firing rates are selected preferentially by the attention system. The model correctly reproduces some observations concerning the mechanisms of attentional control, such as the coherence of spikes in the population of neurons included in the focus of attention, and the inhibition of neurons outside the focus of attention. Sequential selection of stimuli simultaneously present in the visual scene is demonstrated by the model in the frequency domain in both a formal example and a real image.

1. Introduction

Selective visual attention is a mechanism that allows a living organism to select the most important part of the incoming visual information and ignore other parts of the visual stream. This mechanism is necessary due to the limited processing capacity of the nervous system which precludes the analysis of all simultaneously presented stimuli whose significance for the subject varies rapidly. Due to the attentional filter the important stimuli can be processed more carefully and in more detail in a short time.

Visual attention in human and monkey brains is realized by a large-scale distributed neural network that includes several cortical and subcortical areas with bottom–up and top–down flow of information between them (Corbetta, 1998; Knight, 1997). The question of the existence of a hierarchy in the attention system is still unresolved. Some researchers assume that attention is a distributed, self-organized system without any leading structure. Other researchers believe that there is a special central structure (the so-called central executive) that controls the functioning of the attention system and arguments in favour of this hypothesis have been presented in Baddeley (1996, 2002) and Cowan (1988). Recent studies have shown that the central executive may be represented by a distributed network that includes lateral, orbitofrontal, and medial prefrontal cortices linked with motor control structures (Andres, 2003; Barbas, 2000). There is some evidence that in addition to neocortical areas the hippocampus may play an important role in implementing central executive functions: the hippocampus has the uppermost position in the pyramidal structure of convergent cortical zones (Damasio, 1989), participates in controlling the processing of information in most parts of the neocortex (Holscher, 2003), and coordinates the work of the attention system (Herrmann & Knight, 2001; Vinogradova, 2001).

Despite intensive studies of neuronal activity related to attention, it is still unclear what neuronal mechanisms are used by the brain to implement attention. Electrode recordings and functional brain imaging in animals and humans have revealed two types of attentional modulation of neural activity in the cortex. First, increased excitation of neurons representing attended stimuli is observed while neural activity evoked by unattended stimuli is reduced to a low level (McAdams & Maunsell, 1999; Moran & Desimone, 1985). Second, gamma range oscillations correlate with the activity of neurons in the attentional focus (Doesburg, Roggeveen, Kitajo, & Ward, 2008; Tallon-Baudry, Bertrand, Henaff, Isnard, & Fischer, 2005). The coherence of spiking plays a major role in the control of attention (Fell,

* Corresponding author at: Centre for Theoretical and Computational Neuroscience, University of Plymouth, Plymouth PL4 8AA, UK. Tel.: +44 1752232619; fax: +44 1752232541.
E-mail addresses: david.chik@plymouth.ac.uk (D. Chik), r.borisyuk@plymouth.ac.uk (R. Borisyuk).

0893-6080/$ – see front matter © 2009 Elsevier Ltd. All rights reserved.
doi:10.1016/j.neunet.2009.02.002

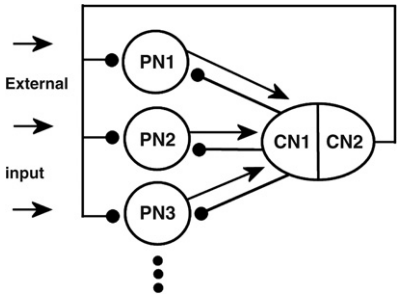

Fig. 1. The connection architecture of the attention model. PN1, PN2, PN3, ... are peripheral neurons encoding the features of external stimuli. CN1 and CN2 are central neurons which control the attention focus. Excitatory connections are shown by arrows, inhibitory connections are shown by lines with black circles at their ends.

Fernandez, Klaver, Elger, & Fries, 2003; Fries, Schroeder, Roelfsema, Singer, & Engel, 2002; Singer, 1999; Steinmetz et al., 2000).[1] The latter evidence is considered to support the temporal correlation hypothesis (Gray, 1999; von der Malsburg, 2001) i.e. increased synchrony can reinforce the impact of spikes on subsequent cortical areas. It is reasonable to expect that models of attention should be able to reproduce these results using biologically plausible neural networks.

The temporal correlation theory has been used as the basis for several models of attention. Niebur and Koch (1994) have presented a model for the experimental data of Moran and Desimone (1985) recorded from the striate (V2) and extrastriate (V4) areas of the neocortex. In this model visual attention is interpreted as a local correlation of Poisson processes in V2. The covariant activity increases the firing rate of a local population of neurons and the coincidence detector in V4 suppresses the activity of V4 cells associated with unattended stimuli. Corchs and Deco (2001) developed a model of visual conjunction-feature search (Chelazzi, Miller, Duncan, & Desimone, 1993; Treisman & Gelade, 1980) where attentional bias was modulated by top–down signals, from memory that coded target feature values, to feature processing structures in the primary areas of the visual cortex.

An oscillatory model of attention comprising a layer of the so-called peripheral oscillators interacting with a special central oscillator has been developed in a series of papers (Borisyuk & Kazanovich, 2004; Kazanovich & Borisyuk, 1994, 1999, 2003). Advanced phase oscillators have been used as the elements of this model. The state of such an oscillator is described by three variables: phase, amplitude, and natural frequency of oscillations. The functioning of the model has been based on the following main principles: (1) partial synchronization between the central oscillator and some subset of peripheral oscillators and (2) resonant increase of the amplitude during partial synchronization. The phase-locking mechanism used to synchronize oscillators allows them to achieve similar frequencies and the focus of attention is assumed to be formed by those peripheral oscillators whose activity is partially synchronous with the activity of the central oscillator.

The model we propose here aims to elucidate the problem of how selective attention operates through the spiking dynamics of neurons, in particular, how selective attention can be represented by the synchrony and suppression of neural activity in a network of interactive spiking elements. The model consists of a layer of non-interacting neurons (peripheral neurons) and two central neurons (CN1 and CN2) with global feedforward excitatory and feedback inhibitory connections between peripheral neurons and CN1, and global inhibitory connections from CN2 to peripheral neurons (Fig. 1). Peripheral neurons code the features of objects and are assumed to be located in the primary visual cortex. Partial synchronization of a subgroup of peripheral neurons with CN1 is interpreted as the formation of the attention focus. CN2 provides additional inhibition to peripheral neurons and switches the attentional focus between objects.

The model uses biologically derived Hodgkin–Huxley neurons as basic elements which are coupled according to an attention-related architecture. The dynamical properties of such a network as well as the performance of the model in solving selective attention tasks have not been previously investigated. The model allows us to characterise the formation of the focus of attention in terms of the spiking activity of individual neurons and the coherent spiking of neuronal assemblies instead of employing coarse level modelling of oscillators representing the population spiking rate. The advantage of this approach is that the model provides information on the activity of single neurons and the type of synchronization appearing between the neurons during the attention state on a real time scale and under physiologically plausible parameter values. Therefore it is possible to make a better comparison between the simulated neural dynamics and experimental recordings of spiking activity.

Although our previous experience has shown that an architecture with a central element can be helpful for attention modelling, we found that the transformation of this type of model into a network of spiking neurons is a difficult task. The system includes many parameters and it is not clear *a priori* how to define their values to obtain desirable neural dynamics. We employ a mixture of simulations and numerical bifurcation analysis to study the regimes of synchronous dynamics associated with formation of the attention focus. To find the correspondence between parameter values and dynamical modes, we investigated a simplified system formed by a central neuron and two peripheral neurons. Using bifurcation analysis, we found the boundaries in parameter space which separate the regimes of global and partial synchronization. This bifurcation analysis was found to be useful in providing initial values for parameters which were further adjusted in simulations.

The study of the model revealed several dynamical regimes associated with different aspects of the development of the attentional focus including partial synchronization and transitional forms of synchronous dynamics. The boundaries in parameter space between regions with different dynamical behaviour have been computed. It is shown that peripheral neurons with the highest firing rates are preferentially selected by the attention system. We demonstrate the performance of the model by applying it to a real image from a still camera that contains three objects with different colours. It is shown that the model reproduces some basic experimental results concerning the mechanisms of attentional control (gamma range spiking activity, coherence of spikes in the attention focus, suppression of the activity corresponding to unattended stimuli, etc.). The results of these simulations may be useful for the formulation of new hypotheses about the neural mechanisms of attention that will be tested in future experiments.

The model description is provided in Section 2. We investigate the dynamics of the model in Section 3. Simulation results are presented in Section 4. Section 5 is devoted to the discussion of the results and comparison with experimental data.

2. Model description

The two-layer architecture of the model connections is shown in Fig. 1. Peripheral neurons (PNs) represent feature detectors in the primary areas of the neocortex that are activated by external stimuli. It is assumed that the external input to PNs is sufficiently

[1] In Discussion we review the experimental evidence on attention and compare it with the results of model simulations.

large to cause their firing at some particular frequency. In the case of visual attention modelling, the input is an image on a plane grid. The PNs are located on another grid of the same size as the image, with each PN receiving a signal from the pixel whose location on the grid is identical to the location of the PN. In general, the PNs should be bound by excitatory lateral connections but to facilitate the analysis of the model dynamics these connections are currently not considered. The only connections that are present in the model are the connections between the PNs and the central unit.

The central unit is an extremely simplified version of the central executive. It consists of two neurons, CN1 and CN2. CN1 enables attention to be focused on a selected subset of PNs. CN2 controls the shift of attention from one stimulus to another. This allows CN1 to consecutively synchronize its firing with different assemblies of PNs. Both CN1 and CN2 send inhibitory signals to all PNs, but excitatory input signals from PNs are received by CN1 only. In this study, we assume that the connection strengths between CN1 and all PNs are constant and universal. There are no connections between CN1 and CN2.

The strength of inhibition from CN1 is fixed but inhibitory signals from CN2 vary over time. We suppose that there is a short-term plasticity in the strength of the connection from CN2 to each PN. If both neurons have high activity for a prolonged time, the inhibitory synapse will be strengthened, while if either one of them has low activity the synaptic strength will decay (Fitzpatrick, Akopian, & Walsh, 2001; Zucker & Regehr, 2002). The PNs that are currently selected by CN1 may be suppressed by CN2. This provides CN1 with an opportunity to change the focus of attention by synchronizing its activity with another assembly of PNs. The introduction of an inhibitory influence from CN2 to PNs reflects the experimental evidence that attention is biased against returning to previously attended stimuli (Klein, 1988; Takeda & Yagi, 2000).

The Hodgkin–Huxley model (Hodgkin & Huxley, 1952) is employed for each neuron. It is described by the following equations:

$$\frac{dV}{dt} = -I_{ion} + I_{ext} - I_{syn}, \tag{2.1}$$

$$\frac{dX}{dt} = A_X(V)(1-X) - B_X(V)X, \quad X \in \{m, h, n\}, \tag{2.2}$$

where V is the membrane potential of the neuron, m, h, n are the gating variables of the ionic channels, and I_{ion} denotes the ionic current which is given by

$$I_{ion} = g_{Na}m^3h(V - V_{Na}) + g_K n^4(V - V_K) + g_L(V - V_L), \tag{2.3}$$

where g_{Na}, g_K, g_L are the maximum conductances for the sodium, potassium and leak currents, respectively, V_{Na}, V_K, V_L are the corresponding reversal potentials. All details of the model including description of variables and specifications of all parameter values can be found in Appendix A.

External stimulation of a PN is represented by the current

$$I_{ext}(t) = \tilde{I}_{ext}(1 + 0.01\xi(t)), \tag{2.4}$$

where $\tilde{I}_{ext}$ is a constant and $\xi(t)$ is a random process without time correlation and the random variables $\xi(t)$ are identically and uniformly distributed in $[-1, 1]$. The current $\tilde{I}_{ext}$ is suprathreshold and induces an intrinsic firing rate for each PN. We assume that different features of a stimulus are coded by different values of $\tilde{I}_{ext}$, hence PNs utilize frequency coding. For example, in the case of a visual stimulus the value of $\tilde{I}_{ext}$ may be determined by the colour of the pixel.

The random process $\xi(t)$ can be considered as an additive noise in the system. The purpose of adding a small noise is to break the symmetry and introduce heterogeneity in order to guarantee that the final state of the network will be a global attractor. Also, some parameter values of each PN have been randomised (see Appendix A). However, the dynamics of the model are robust and have not been influenced.

It is not necessary for CN1 to receive an external current to generate action potentials. If the excitatory inputs from PNs to CN1 are strong enough, they will force CN1 to fire. If CN1 already has an intrinsic firing rate, then the excitatory input will increase its firing rate even further. In contrast, CN2 requires an external current, otherwise it would be silent. In our simulations, the standard external input I_{ext} to CN1 is 5 mA and that to CN2 is 30 mA.

The interaction of the neurons is expressed by the synaptic current I_{syn}. In our model, CN1 receives excitatory synaptic inputs from all PNs, while CN2 does not receive any synaptic input from other units (it receives an "external" current that could represent areas within the brain that are not directly involved in the attention mechanism). PNs receive inhibitory inputs from both CN1 and CN2. The equations are described below.

2.1. Excitatory connections from PNs to CN1

The excitatory synaptic current I_{syn} received by CN1 from PNs is

$$I_{syn} = w_1(V - V_{syn,exc}) \sum_{j=1}^{N} \sum_{k=1}^{M_j} \alpha_{exc}(t - T_{j,k}). \tag{2.5}$$

Here V is the potential of CN1, w_1 denotes the connection strength from a PN to CN1, which is constant and universal for all PNs, $V_{syn,exc}$ is the synaptic reversal potential for excitatory connections (in simulations $V_{syn,exc} = 0$ mV), and $\alpha_{exc}(t)$ represents the synaptic conductance: $\alpha_{exc}(t) = at\exp(-bt)$ for $t \geq 0$ and zero for $t < 0$ is the alpha-function of excitatory coupling with parameters a and b controlling the shape of the alpha-function (in our simulations $a = 2\ \text{ms}^{-1}$, $b = 0.1\ \text{ms}^{-1}$), $T_{j,k}$ is the time of the kth spike generated by the jth PN. The first summation refers to all spike times of the jth PN (M_j is the total number of spikes generated by the jth PN). The second summation refers to synaptic inputs from all neurons (N is the total number of PNs).

2.2. Inhibitory connections from CN1 and CN2 to PN

We suppose that the ith peripheral neuron receives inhibitory synaptic currents from the central units CN1 and CN2:

$$I_{syn,i} = w_2(V_i - V_{syn,inh}) \sum_{k=1}^{M_2} \alpha_{inh}(t - T_k) + w_{3,i}(t)(V_i - V_{syn,inh}) \sum_{k=1}^{M_3} \alpha_{inh}(t - S_k), \quad i = 1, 2 \ldots, N. \tag{2.6}$$

Here $V_i(t)$ is the potential of the ith PN, w_2 is the connection strength (maximal synaptic conductance) from CN1 to PN, which is constant and universal for all PNs, M_2 is the total number of spikes of CN1, M_3 is the total number of spikes of CN2, T_k is the time of the kth spike generated by CN1, S_k is the time of the kth spike generated by CN2, and $V_{syn,inh}$ is the synaptic reversal potential of inhibitory coupling (in simulations $V_{syn,inh} = -80$ mV for all PNs). The alpha-function $\alpha_{inh}(t)$ represents inhibitory synaptic conductance and has the same form as $\alpha_{exc}(t)$ with the parameters $a = 0.6\ \text{ms}^{-1}$, $b = 0.03\ \text{ms}^{-1}$.

In Eq. (2.6), $w_{3,i}(t)$ is the modifiable GABAergic connection strength from CN2 to the ith PN, representing the short-term plasticity:

$$w_{3,i}(t) = \begin{cases} \tilde{w}_3, & T_{H,i} \leq t \leq T_{H,i} + \Delta h \\ 0, & \text{otherwise,} \end{cases} \tag{2.7}$$

where $\tilde{w}_3$ is the saturation value of plasticity, $T_{H,i}$ marks the onset time of plasticity, and Δh represents the duration of plasticity

(a fixed parameter). The decay of the connection strength can be motivated by a limited store of releasable neurotransmitters such that the synapse will be disabled after prolonged activation (Brager, Capogna, & Thompson, 2002). The plasticity can also decay due to homeostasis, anti-Hebbian property, or other decay mechanisms. Here we assume that $w_{3,i}(t)$ drops back to zero after decay, that is, after the time Δh has expired.

Let $T_{R,i}$ be the time of the previous reset of the plastic connection from CN2 to the ith PN, i.e. the time when $w_3(t)$ last decayed to zero. The onset time of plasticity $T_{H,i} > T_{R,i}$ is determined as the first time moment that satisfies the following equation:

$$\int_{T_{R,i}}^{T_{H,i}} \Theta(V_i(t) - \upsilon) \cdot \Theta(V_{CN2}(t) - \upsilon) \mathrm{d}t = \frac{1}{\varepsilon}, \tag{2.8}$$

where υ is the threshold value for detecting spike generation, ε is a parameter ($0 < \varepsilon < 1$), and

$$\Theta(x) = \begin{cases} 1, & x > 0 \\ 0, & x \leq 0. \end{cases} \tag{2.9}$$

The value on the left-hand side of Eq. (2.8) measures how often the spikes of the ith PN and CN2 coincide in time. As soon as this value reaches the threshold $1/\varepsilon$, the connection strength jumps up to the saturation level $w_{3,i}(t) = \tilde{w}_3$. The period of saturation lasts for Δh ms. After that time the connection strength $w_{3,i}(t)$ drops to zero and the process of connection modification starts a new cycle. Such modification process can be considered as an approximation of Hebbian learning. The simplification is in postulation of abrupt jumps (up and down) of the connection strength instead of gradual increase and decrease. More explanations on how this approximation has been obtained are presented in Appendix B.

During the simulation, all equations are numerically integrated using the fourth-order Runge–Kutta method.

3. Synchronous dynamics

According to our assumption, the focus of attention is formed by those PNs which spike synchronously with CN1. Therefore it is important to investigate the dynamical regimes of the model. We distinguish five types of dynamics: global synchronization, partial synchronization, transitional state, quiescence, and asynchronous state. The following examples illustrate the conditions under which these types of dynamics can appear. The neuron CN2 is not essential for attention focusing because the role of this neuron is to switch attention between objects in the visual scene. In this section we consider simulations without attention switching.

Intensive study of dynamical regimes and synchronization was undertaken in application to the model containing CN1 and 200 PNs. The PNs were arranged into two groups with one group having a stronger external input and consequently a higher frequency of spike generation. To illustrate the results of our study, we limit the number of PNs to 10. The model with this reduced number of PNs exhibits the same qualitative behaviour as in the case of 200 PNs.

Let us distribute 10 PNs between two groups A and B with 5 PNs in each group. The mean values of external currents for the groups A and B are I_1 and I_2, respectively ($I_1 > I_2$). The neuron CN1 receives an external current of 5 mA; this is lower than both I_1 and I_2.

If all connections are neglected ($w_1 = w_2 = w_3 = 0$), all PNs would fire independently at different frequencies (determined by the values of external currents). This state of independent spiking is called the ***asynchronous state***. Note that CN1 would not fire (unlike PNs) because it receives a subthreshold external current.

In the regime of ***global synchronization*** (Fig. 2), all PNs generate spikes coherently with CN1 in the ratio 1:1. Notice that CN1 is now firing due to the excitatory inputs from PNs. This regime is stable if the inhibitory influence of CN1 on PNs is not too strong.

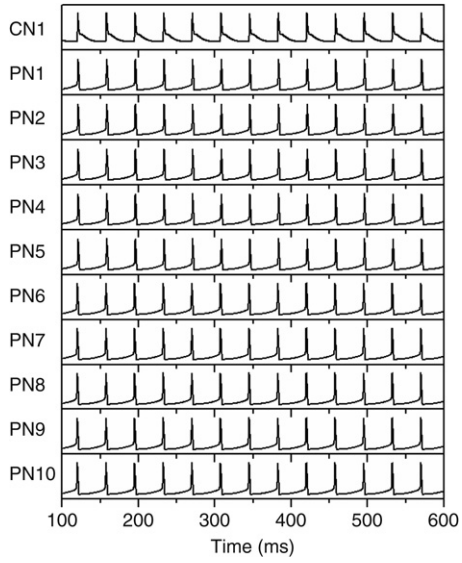

Fig. 2. Global synchronization. The panels show the potential traces of different neurons. Input current to CN1 is 5 mA, $I_1 = 25$ mA, $I_2 = 27$ mA. Connection strengths are $w_1 = 0.1$, $w_2 = 0.5$, $w_3 = 0$.

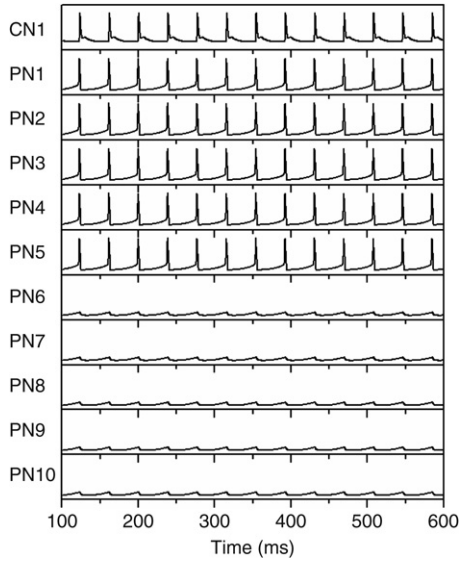

Fig. 3. Partial synchronization. The panels show the potential traces of different neurons. Input current to CN1 is 5 mA, $I_1 = 25$ mA, $I_2 = 11$ mA. Connection strengths are $w_1 = 0.1$, $w_2 = 0.5$, $w_3 = 0$.

In the regime of ***partial synchronization*** the neurons of one group generate spikes coherently with CN1 while the neurons of the other group do not generate spikes. Fig. 3 shows the situation when the neurons of group A are in partial synchronization with CN1. For neurons of group B, the fluctuations of the membrane potential are synchronized with the spikes of CN1, but the amplitude of these fluctuations is too small to generate a spike. The regime of partial synchronization appears if the inhibitory influence of CN1 on PNs is strong enough. We interpret this situation as the concentration of attention on a stimulus represented by the neurons of group A. Thus, the regime of partial synchronization is used to represent selective attention.

The ***quiescence*** regime appears if the inhibitory influence of CN1 on PNs is strong (especially when the external current to CN1 is suprathreshold). In this mode all spiking activity of neurons in both groups A and B is suppressed, however, the membrane potentials oscillate synchronously with the spikes of CN1.

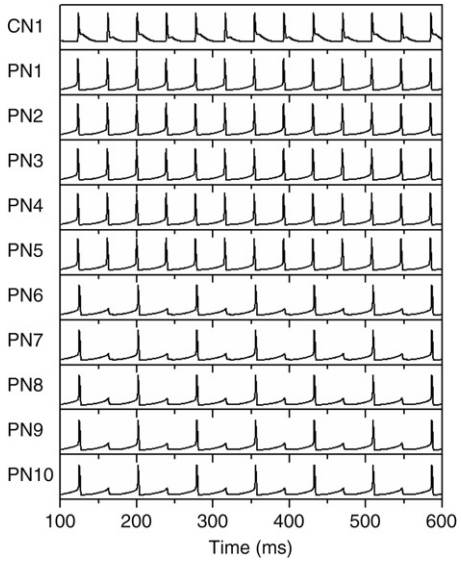

Fig. 4. Transitional state. The panels show the potential traces of different neurons. Input current to CN1 is 5 mA, $I_1 = 25$ mA, $I_2 = 22$ mA. Connection strengths are $w_1 = 0.1$, $w_2 = 0.5$, $w_3 = 0$.

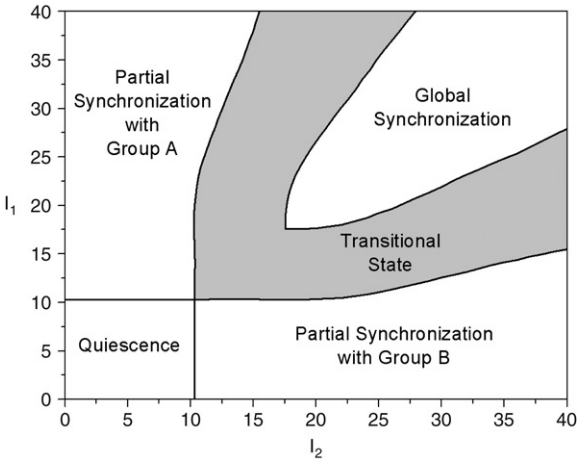

Fig. 5. Dynamical profile of the system with two groups of PNs. The axes show I_1 and I_2 which determine the intrinsic frequencies of groups A and B, respectively. The dynamical behaviours are labelled as: global synchronization, transitional state, partial synchronization and quiescence. Input current to CN1 is 9.8 mA. Connection strengths are $w_1 = 0.002$, $w_2 = 0.4$, $w_3 = 0$.

Our simulations show that the transition from global to partial synchronization and then to the quiescent state caused by parameter variation does not happen as a sudden jump but passes through the so-called ***transitional state.*** In this regime the peripheral neurons are neither fully synchronized with CN1 nor quiet. Fig. 4 presents an example of spiking activity during the transitional state. In this example, the neurons in group A fire coherently with CN1, but the spikes of the neurons in group B are phase-locked with CN1 in ratio 1:2 (one spike is regularly missing as shown by the smaller, subthreshold peaks). It should be noted that the firing of neurons in group B might be incoherent. For example, in Fig. 4 neurons PN7 and PN9 fire in anti-phase with other members of group B. In general, the behaviour of a single neuron in group B can be characterised in the following way: the neuron sometimes produces a spike almost coherently with a spike of CN1 and sometimes skips a spike. For example, a PN can generate 3 spikes synchronously with CN1 but then skips a spike. Also, many other spiking patterns of synchronous and missing spikes have been observed. Different spiking patterns may coexist in the transitional state. For example, spiking patterns with the ratio 2:1 (two spikes of CN1 and 1 spike of the neurons in group B) and with the ratio 3:2 coexist for some parameter values. We interpret these multiple patterns of spiking in the transitional state as different degrees of attention concentration.

The variety of dynamical regimes is not limited by periodic and quasi-periodic modes. Irregular chaotic activity is also possible. For example, using parameters $\tilde{I}_{CN1} = 9.8$ mA, $I_1 = 25$ mA, $I_2 = 11$ mA, $w_1 = 0.002$, $w_2 = 0.071$, $w_3 = 0$, the system demonstrates chaotic behaviour. To confirm this fact, we calculated the Lyapunov exponent, which was found to be 0.01.

Fig. 5 shows a diagram (similar to the bifurcation diagram) representing the boundaries between different dynamical regimes in the 2D space of parameters I_1 and I_2 which define the intrinsic frequencies of PNs in groups A and B, respectively. The input to CN1 is suprathreshold. If both currents are large enough, the regime of global synchronization takes place. If both currents are small enough, all PNs are in the quiescent regime. The boundaries shown in Fig. 5 have been determined by multiple simulations of the system.

The diagram shows that if both groups A and B have high intrinsic frequencies (both I_1 and I_2 are large) the whole system is in the global synchronization state. Decreasing either I_1 or I_2 transfers neural dynamics to the transitional state which is characterised by diversity of periodic spiking patterns. For example, one can see a pattern with a skipped spike in group B among 10 consequent spikes of CN1, or a skipped spike among nine spikes of CN1, etc. Also, there is a subregion of the transitional state with irregular chaotic dynamics.

Let us fix the value of the parameter $I_1 = 35$ and gradually decrease the value of the parameter I_2 starting from $I_2 = 35$. The following sequence of transformations of dynamical behaviour can be observed: (1) global synchronization between CN1 and all PNs with 1:1 spike ratio ($24 < I_2 < 35$); (2) variety of spiking patterns both periodic and irregular, CN1 is in 1:1 spike ratio with group A and some spikes of neurons in group B are skipped ($14 < I_2 < 24$); (3) partial synchronization with neurons of group A ($0 < I_2 < 14$).

The diagram in Fig. 5 has been obtained by numerical study of the system. A more rigorous approach based on bifurcation analysis and accurate calculation of limit cycles and their stability has also been used. The parameter region corresponding to the transitional state is not narrow and contains limit cycles (both stable and unstable) of different shapes corresponding to different spiking patterns. The transition from global to partial synchronization involves a number of bifurcations of limit cycles. Suppose that the limit cycle with 1:1 spiking pattern corresponds to the regime of partial synchronization and other multiple limit cycles correspond to partial synchronization with different patterns of missing spikes (e.g. each second spike is missing, or each third spike is missing, etc). We used MATCONT software (freely available from http://www.matcont.ugent.be) for continuation of the limit cycle within parametric space and studied the limit cycle bifurcations in the transitional state between global and partial synchronization. This investigation shows a very complex structure of multiple bifurcations of limit cycles near the boundaries of the transitional zone. The typical bifurcation is the fold bifurcation of the limit cycle (stable and unstable limit cycles merge and disappear). In the usual scenario, the limit cycle corresponding to partial synchronization with some particular pattern of missing spikes is stable and undergoes only slight changes until a critical value of parameters is reached where branches of stable and unstable limit cycles merge and both limit cycles disappear. In spite of intensive study of bifurcations of limit cycles in the transitional state, there remain many uncertainties about the complete bifurcation structure of the model, therefore further investigations are required.

An important result of these simulations is that selective attention (associated with partial synchronization) always favours a group with higher frequency. If group A has a higher intrinsic frequency ($I_1 > I_2$) then group A will be engaged in the regime of partial synchronization (and vice versa). This is also true if the number of groups is higher than two. In neurophysiology, higher salience of a stimulus is usually revealed in a higher level of neural activity representing this stimulus in the cortex. Therefore the model complies with the fact that the most salient stimulus should have the priority in being selected in the focus of attention.

4. Selective attention

In this section we demonstrate how the model performs sequential selection of objects in the focus of attention. Two examples are considered. In the first example we deal with a population of spiking PNs with uniformly distributed frequencies. We demonstrate that the model automatically selects the subgroup containing the fastest neurons and includes them into the attention focus. In terms of neural dynamics this means that the PNs in the selected subgroup generate spikes synchronously with CN1 in the gamma range, while other PNs do not fire. Due to the Hebbian type learning rule, the strength of inhibitory connections from CN2 to the selected subgroup gradually increases. As a result, spike generation in the selected subgroup is stopped. This developed inhibition lasts for some time preventing the neurons from the inclusion in the focus of attention. In the mean time the focus of attention moves to the second fastest subgroup of PNs, etc. The neurons of the previously selected subgroup will again be eligible for inclusion in the focus of attention after some interval which depends on the rate of decay of the synaptic inhibition from CN2. The second example illustrates the system performance in the case of a real visual scene with three objects recorded by a still camera.

4.1. Example 1

Let us consider a model with 80 PNs with input currents distributed in the interval [10, 50] mA. The external inputs to CN1 and CN2 are 5 mA and 30 mA, respectively. Fig. 6 demonstrates the distribution of the intrinsic frequencies: the spiking rastergram of PNs is shown for the case of disabled connections from the central neurons. The PNs marked by lower numbers have shorter firing periods (higher intrinsic frequencies) therefore they have a better chance for earlier inclusion in the attention focus.

Fig. 7 presents the rastergram of PNs in the case when all connections with the central neurons are restored. It shows that the population of PNs is split into five subgroups that are consecutively synchronized by CN1. The process starts from the group with the highest intrinsic frequency (neurons from PN1 to PN16). During the time interval 0–120 ms this group operates in the regime of partial synchronization with CN1. During the next time interval from 120 to 240 ms another group is included in the regime of partial synchronization with CN1, etc. The selection of a group in the regime of partial synchronization and the corresponding shift of attention are controlled by CN2 through the short-term plasticity between CN2 and PNs. The parameters of plasticity are chosen in such a way that after a PN generates five spikes the inhibitory connection from CN2 to this PN is activated which results in the activity of the PN being shut down. The plasticity decays after 650 ms so that the selection cycle can be continuously repeated.

Although there are no direct connections between PNs, they are automatically split into five groups. Since the original input currents vary gradually among the PNs, the grouping somehow represents the resolution of the signal and this resolution depends on the system parameters and can be adjusted. In Section 3, we have shown that the boundary between two regimes of partial synchronization of different groups is not a line but a region with intrinsic frequencies of neurons belonging to the transitional state.

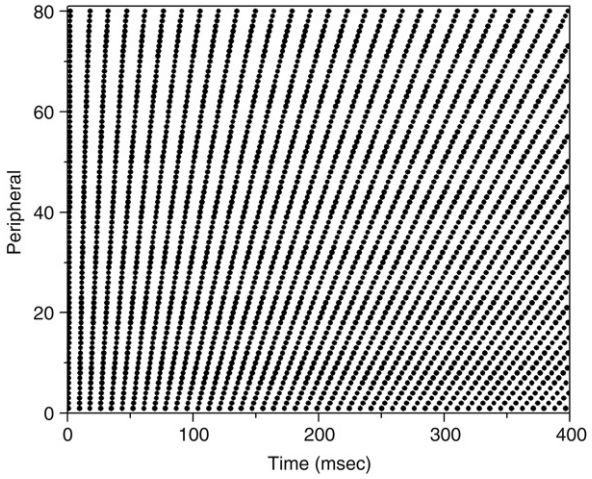

Fig. 6. Rastergram (spikes of neurons versus time) of 80 disconnected PNs (the vertical axis represents the number of the peripheral neuron). Each black dot represents a single spike of a neuron. Input to CN1 = 5 mA, input to CN2 = 30 mA, inputs to PNs vary to provide different intrinsic frequencies. Connection strengths are $w_1 = w_2 = w_3 = 0$.

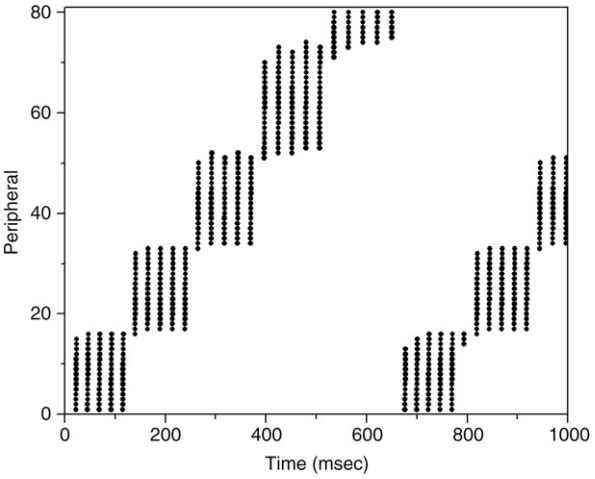

Fig. 7. Rastergram (spikes of neurons versus time) corresponding to sequential selection (the vertical axis represents the number of the peripheral neuron). Each black dot represents a single spike of a neuron. Inputs to CN1 and CN2 and external current inputs to PNs are the same as in Fig. 6. Connection strengths are $w_1 = 0.1$, $w_2 = 9$, $w_3 = 5$. Other parameters are $\upsilon = -10$ mV, $\Delta h = 650$ m s, $\varepsilon = 0.16$/ms.

This explains an interesting behaviour of some neurons which are selected in both of the two adjacent subgroups. An example of such a neuron can be found in Fig. 7: the neuron PN73 is selected in both of the subgroups 4 and 5.

Fig. 7 also shows that partial synchronization occurs in the gamma range of around 35 Hz. The first selected subgroup (PN1–PN16) oscillates at around 40 Hz which is higher than the last selected subgroup (PN74–PN80) oscillating at around 30 Hz.

4.2. Example 2

To demonstrate model performance in the case of a real visual scene, we use a still camera image that contains three objects: an orange, a pear, and a blue cloth. The objects are placed on an almost white background. A grid of 320 × 240 PNs was used in the simulation, providing a one-to-one correspondence between the PNs and the pixels of the image which is also of the size 320 × 240. We suppose that different colours are encoded as different intrinsic

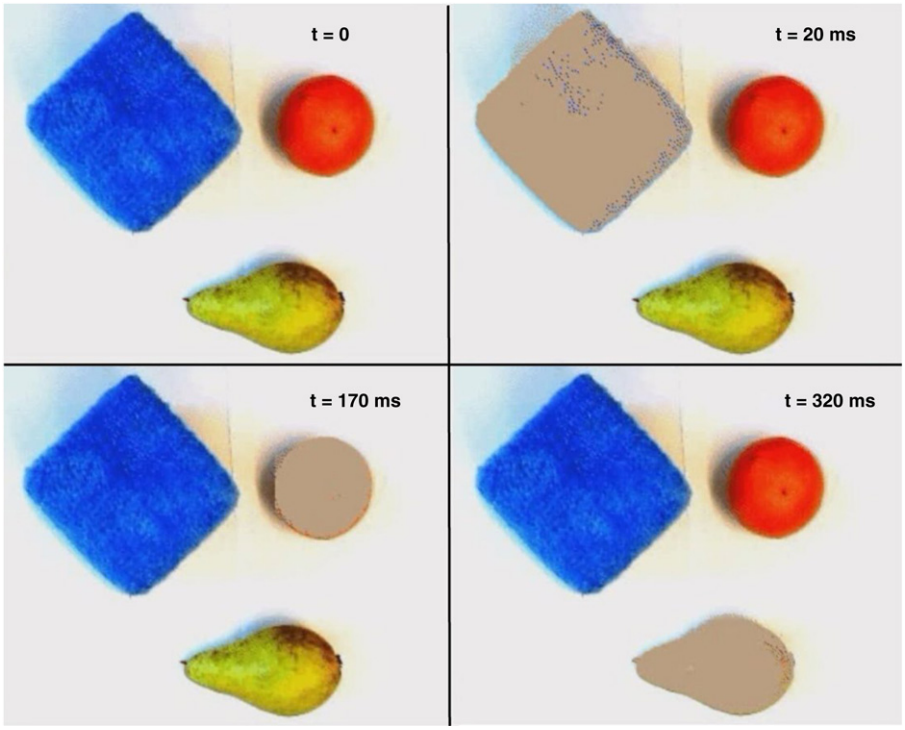

Fig. 8. Sequential selection of objects in a real image (the original AVI movie can be found at http://www.pion.ac.uk/binmam/). PNs have one-to-one correspondence with image pixels. The fawn area indicates the location of active PNs. The colour values of image pixels are converted to external current values of PNs. Input to CN1 $= 5$ mA. Input to CN2 $= 30$ mA. Connection strengths are $w_1 = 0.1$, $w_2 = 9$, $w_3 = 5$. Other parameters are $\upsilon = -10$ mV, $\Delta h = 650$ m s, $\varepsilon = 0.16$/ms.

frequencies of PNs. We linearly converted the RGB values of pixels into the values of the external current $\tilde{I}_{ext}$ in the range 10–40 mA.

The results of these simulations are presented in Fig. 8. The firing frequencies are in the gamma range (around 40 Hz). An overlay is used on top of the image to mark the currently attended area: if a PN fires then the corresponding pixel is coloured in fawn. During the time interval 0–20 ms there is a transitory period when no selection of objects occurs. At $t = 20$ ms, the cloth is selected. At this moment the system is in the regime of partial synchronization between CN1 and the PNs located in the cloth area. Other PNs are all suppressed. The selection of the cloth continues until the moment $t = 170$ ms when the orange is selected. Then at $t = 320$ ms the pear is selected. After that the focus of attention returns back to the cloth, etc.

The formation of the attentional focus is controlled by CN1. At any moment one assembly of PNs has higher frequency than the other two assemblies and this assembly of neurons is selected first. The shift of attention to another object is controlled by CN2 which increases its inhibitory influence on the firing PNs and keeps this inhibition for some time. During this period inhibited PNs cannot generate spikes but they return back to the normal spiking regime after the inhibitory period has expired.

5. Discussion

We developed and studied a new model of selective visual attention based on two-layer architecture, consisting of a layer of non-interacting neurons with global feedforward excitatory and feedback inhibitory connections to two central neurons. This model consists of spiking neurons of Hodgkin–Huxley type with meaningful neurobiological parameters. The advantage of this new model is that the direct comparison with experimental recordings of spiking activity is allowed.

We have shown that an inhibitory neuron connected to an assembly of spiking neurons is able to synchronize their activities. The type of synchronization depends on the connection strengths and the distribution of intrinsic spiking frequencies. Analysis of the model revealed five regimes of synchronous dynamics that can be associated with the attention focus: global synchronization, partial synchronization, transitional state, quiescence, and asynchronous state. The bifurcation diagram and the boundaries in the parametric space between the regions of different dynamical modes have been calculated. It has been shown that peripheral neurons with the highest firing rates are preferentially selected by the attention system.

The model can sequentially select separate objects simultaneously presented in the visual scene. To test model performance, we used a formal example and a real image from a still camera that contained three colour objects on a white background. Simulations confirmed that there is a reliable shift of attention from one object to another due to a properly tuned mechanism of Hebbian-type learning that allows the system to avoid focusing attention repeatedly on the previously selected object.

The robustness of the model has been carefully checked. The values of some parameters (e.g. maximum conductance of each channel) have been randomised and the random addition for each PN has been chosen in the range $\pm 2\%$. We found that such parameter perturbation does not destroy the dynamical behaviour of the model. Also, the uniform noise of the order of 1% of the external current has been added to the right-hand side of the equation describing the dynamics of the potential. For each moment of time the random addition is uniformly distributed in the range $\pm 1\%$ of the value of the external current. It was found that this level of the noise does not change the dynamics of the model. Note that we have used an extremely strict definition for partial synchronization. The suppressed group should fire no spikes at all while the spikes of the selected group should be coherent and in one-to-one correspondence with the spikes of the central neuron. In the real attention system, one can expect a more stochastic type of synchrony reflected in the correlation of spike flows. Under these milder conditions, introduction of a rather large noise in the model will have no significant effect on the selection performance as long as the mean external inputs for different objects have large enough difference.

5.1. Comparison with other attention models

Katayama, Yano, and Horiguchi (2004) suggested a selective attention model based on a two-layer network of Hodgkin–Huxley neurons. Their main results partly coincide with ours: (a) synchronous firing of neurons in the second layer with a subset of neurons in the first layer, (b) rapid shift of attention from one object to another. However, due to the lack of inhibitory connections in their model, object selection is not an automatic dynamical process but is implemented by manually setting the proper values of input currents.

Tiesinga (2005) published a model based on Hodgkin–Huxley type neurons which reproduced experimental results about the response of V4 neurons when attention shifts between two stimuli. In our model, however, we concentrate on the higher level implementation of selective attention and a possible mechanism of interaction between the higher and lower cortical areas. Note also that in contrast to Tiesinga's model our model can operate with more than two competing objects.

An architecture with an inhibitory central unit has been used by Wang and Terman (1995, 1997) in the network LEGION. The main function of LEGION is image segmentation with the consecutive selection of objects, but in the paper (Wang, 1999) a modification of LEGION oriented towards attention modelling was presented. LEGION is designed as a network of Van der Pol oscillators, therefore it is difficult to compare its temporal characteristics (such as the working frequency, the speed of attention focusing, etc.) with experimental data. The consecutive selection of objects is represented by activity in different phases within one oscillation cycle, but in our model the duration of selection is independent of the firing frequency of individual neurons. Also in LEGION, if a single object is included in the focus of attention, the capability of selecting another object will disappear. Finally, in LEGION the largest objects are selected preferentially while in our model the object coded by the highest frequency is selected first. This coding is more flexible and in better agreement with the idea of saliency.

5.2. Comparison of modelling results with experimental data on neuronal mechanism of attention

Let us summarise the most important new findings of our attention model and compare them with what is known from experimental evidence. We first formulate a feature of the model and then present the experimental finding in support of it.

A. The working frequency of synchronization associated with attention belongs to the gamma range.

The same frequency range was observed in many experiments on attention. Fries, Reynolds, Rorie, and Deimone (2001) recorded multi-unit activity and local field potentials in the extrastriate area V4 when a monkey switched attention between visual stimuli and distractors. It was found that neurons activated by the attended stimulus showed increased gamma-frequency synchronization (35–90 Hz) compared with neurons at nearby sites activated by distractors. In similar experiments (Taylor, Mandon, Freiwald, & Kreiter, 2005) attention significantly increased oscillatory currents underlying the recorded field potentials in the gamma range and increased the level of synchronicity of V4 neurons representing the attended stimulus. It is interesting that misdirection of attention to a distractor was preceded by a corresponding shift of oscillatory activity from the neuronal population representing the target to the population representing the distractor. Vidal, Chaumon, O'Regant, and Tallon-Baudry (2006) recorded magnetoencephalogram signals while manipulating the focusing of attention and found that attention focusing is accompanied by low-band gamma oscillations (44–66 Hz) at parietal locations. Their conclusion is that focused attention relies on gamma-band oscillatory synchrony.

B. In the model, a group of PNs with higher spiking activity has a higher chance of being included in the attention focus.

Experiments show that salient visual stimuli that have the advantage in attracting attention elicit higher activity of neurons (Allman, Miezin, & McGuinness, 1985; Morris, Friston, & Dolan, 1997; Sillito, Grieve, Jones, Cudeiro, & Davis, 1995). Increased saliency (e.g. higher contrast or greater dissimilarity with surrounding objects) results in increased neural activity. It is believed that this content-based modulation of neural activity is caused by long-range horizontal connections in early visual cortex.

C. In the model, synchronization is fast enough in comparison to real times of attention focusing.

Experiments on attention speed show great diversity in the latencies of attention focusing and switching. Typical times are between 50–300 ms depending on the complexity of the task (Carlson, Hogendoom, & Ferstraten, 2006; Egeth & Yantis, 1997). In our simulations, the establishment of partial synchronization starting from some random initial conditions takes about 30 ms, which is fast enough to reserve some time for further information processing in the focus of attention.

D. During partial synchronization the activity of neurons representing unattended stimuli is suppressed.

Physiological studies show that inhibition of the activity of neurons representing unattended stimuli is one of the main mechanisms through which irrelevant information is filtered out (McAdams & Maunsell, 1999; Moran & Desimone, 1985; Vanduffel, Tootell, & Orban, 2000). The model allows different degrees of inhibition from complete suppression of firing in "unattended" neurons to partially suppressed activity when "unattended" neurons fire more rarely than "attended" neurons. Bifurcation analysis shows that the range of parameters supporting the latter dynamics is large enough.

5.3. Neural mechanisms of synchronization in attention modelling

Experimental evidence indicates that attention focusing is related to coherent oscillatory spiking activity in the gamma range. An important question is: what is the neuronal mechanism underlying synchronization? In the paper (Niebur, Hsiao, & Johnson, 2002), two potentially plausible neurobiological mechanisms are discussed that might induce synchrony in a population of neurons: (a) lateral coupling between neurons in the population and (b) a common input to all neurons in the population (e.g. synchrony can be induced by a top–down action potential sent simultaneously to all neurons of the population). The authors note that descending feedback projections existing in many sensory systems provide possible hardware for this mechanism. Our modelling may be considered as an argument in favour of the second hypothesis that synchronization is implemented through top–down signals coming from an inhibitory central unit that in its turn is stimulated by bottom–up excitatory signals.

We wish to remark upon the following feature of our attention model. The working regime of the system can be characterised as functioning near the "critical state". The idea that critical regimes and metastable states are important for brain functioning was the subject of many publications (see for example Kryukov, Borisyuk, Borisyuk, Kirillov, and Kovalenko (1990), recent progress was reported in Borisyuk and Cooke (2007)). In our simulations we have chosen the parameters of a single Hodgkin–Huxley neuron and strengths of their connections in such a way that the system dynamics is close to an Andronov–Hopf bifurcation where both oscillations and steady-state modes exist. This critical regime allowed us to efficiently control the dynamics of individual neurons and of the whole network, switching it between different types of synchronous/asynchronous states as well as between different groups of partial synchronizations.

Acknowledgments

We thank Tom Cooke and Martin Coath for corrections of English. This work was supported by the UK EPSRC (Grant EP/D036364/1), by the Russian Foundation of Basic Research (Grant 07-01-00218) and by the Ministry of High Education and Science of the Russian Federation (Grant 2.1.1/3876).

Appendix A

Below the full description of the model is given, therefore some formulas from the main text will be repeated.

We use the Hodgkin–Huxley model for each neuron. Suppose there are N peripheral neurons and 2 central neurons, then we have a total of $N+2$ neurons. They are described by the following equations:

$$\frac{dV_i}{dt} = -I_{ion,i} + I_{ext,i} - I_{syn,i}, \tag{A.1}$$

$$\frac{dX_i}{dt} = A_X(V_i)(1-X_i) - B_X(V_i)X_i, \quad X_i \in \{m_i, h_i, n_i\}, \tag{A.2}$$

$$A_m(V_i) = (2.5 - 0.1(V_i - V_{rest}))/(\exp(2.5 - 0.1(V_i - V_{rest})) - 1), \tag{A.3}$$

$$A_h(V_i) = 0.07\exp(-(V_i - V_{rest})/20), \tag{A.4}$$

$$A_n(V_i) = (0.1 - 0.01(V_i - V_{rest}))/(\exp(1 - 0.1(V_i - V_{rest})) - 1), \tag{A.5}$$

$$B_m(V_i) = 4\exp(-(V_i - V_{rest})/18), \tag{A.6}$$

$$B_h(V_i) = 1/(\exp(3 - 0.1(V_i - V_{rest})) + 1), \tag{A.7}$$

$$B_n(V_i) = 0.125\exp(-(V_i - V_{rest})/80), \tag{A.8}$$

where $i = 1, 2, \ldots, N$ is used to index PNs, $i = N+1$ indexes CN1, and $i = N+2$ indexes CN2. The meaning of variables and the values of parameters are: $V_i(t)$ is the membrane potential of a neuron, $m_i(t)$ is the activation variable of the sodium conductance channel, $h_i(t)$ is the inactivation variable of the sodium conductance channel, $n_i(t)$ is the activation variable of the potassium conductance channel, $I_{ion,i}(t)$ is the total ionic current, $I_{ext,i}(t)$ is the external current to the neuron, $I_{syn,i}(t)$ is the synaptic current received by the neuron, V_{rest} is the resting potential of the neuron (equal to −65 mV).

Notice that the membrane capacitance is equal to 1, therefore it is not shown in Eq. (A.1).

The sum of ionic currents of the ith neuron is,

$$I_{ion,i} = g_{Na}m_i^3h_i(V_i - V_{Na}) + g_K n_i^4(V_i - V_K) + g_L(V_i - V_L), \tag{A.9}$$

where $i = 1, 2, \ldots, N+2$. The meaning and the values of parameters are: V_{Na} is the reversal potential for the sodium current (equal to 50 mV), V_{K} is the reversal potential for the potassium current (equal to −77 mV), V_{L} is the reversal potential for the leak current (equal to −54.4 mV), g_{Na} is the maximum conductance for the sodium current ($g_{Na} = 120(1+0.02\eta)$ mS/cm^2, η is uniformly distributed in [−1, 1]), g_{K} is the maximum conductance for the potassium current ($g_K = 36(1+0.02\eta)$ mS/cm^2, η is uniformly distributed in [−1, 1]), g_{L} is the maximum conductance for the leak current ($g_L = 0.3(1+0.02\eta)$ mS/cm^2, η is uniformly distributed in [−1, 1]).

The following formulas define the external currents incoming to the peripheral neurons (PNs) and central neurons (CN1 and CN2) respectively:

$$I_{ext,\,i}(t) = \tilde{I}_{ext,i}(1 + 0.01\xi_i(t)), \quad i = 1, 2, \ldots, N, \tag{A.10}$$

$$I_{ext,\,N+1} = \tilde{I}_{CN1}, \tag{A.11}$$

$$I_{ext,\,N+2} = \tilde{I}_{CN2}, \tag{A.12}$$

The meaning of variables and the values of parameters are: $\tilde{I}_{ext,\,i}\,(i = 1, 2, \ldots, N)$ are constants. In our simulations of selective attention, these values are determined by the colour value of the image pixel represented by the PN, $\xi(t)$ is a random process without time correlation and the random variables $\xi(t)$ are identically and uniformly distributed in [−1,1], $\tilde{I}_{CN1}$ is the external current delivered to CN1 (equal to 5 mA unless otherwise specified), $\tilde{I}_{CN2}$ is the external current delivered to CN2 (equal to 30 mA).

The synaptic currents received by the central neurons are described by the following equations,

$$I_{syn,N+1} = w_1(V_{N+1} - V_{syn,\,exc})\sum_{j=1}^{N}\sum_{k=1}^{M_j}\alpha_{exc}(t - T_{j,k}), \tag{A.13}$$

$$I_{syn,\,N+2} = 0, \tag{A.14}$$

where N is the total number of PNs, M_j is the total number of spikes of the jth PN, $T_{j,k}$ is the time of the kth spike generated by the jth PN, $\alpha_{exc}(t) = at\exp(-bt)$ for $t \geq 0$ and zero for $t < 0$ is the alpha-function of excitatory coupling with parameters $a = 2\ \mathrm{ms}^{-1}$ and $b = 0.1\ \mathrm{ms}^{-1}$ providing a physiologically realistic shape of the alpha-function, $V_{syn,exc} = 0$ mV is the synaptic reversal potential of excitatory coupling, $w_1 = 0.1$ (unless otherwise specified) is the connection strength of the synaptic current delivered from a PN to CN1.

The synaptic currents received by peripheral neurons are described by the following equations,

$$I_{syn,i} = w_2(V - V_{syn,inh})\sum_{k=1}^{M_2}\alpha_{inh}(t - T_k) + w_{3,i}(t)(V - V_{syn,inh}) \times \sum_{k=1}^{M_3}\alpha_{inh}(t - S_k), \quad i = 1, 2\ldots, N. \tag{A.15}$$

Here M_2 is the total number of spikes of CN1, M_3 is the total number of spikes of CN2, T_k is the time of the kth spike generated by CN1, S_k is the time of the kth spike generated by CN2, $\alpha_{inh}(t) = at\exp(-bt)$ for $t \geq 0$ and zero for $t < 0$ is the alpha-function of inhibitory coupling with parameters $a = 0.6\ \mathrm{ms}^{-1}$ and $b = 0.03\ \mathrm{ms}^{-1}$ providing a physiologically realistic shape of the alpha-function, $V_{syn,inh} = -80$ mV is the synaptic reversal potential of inhibitory coupling, $w_2 = 9$ (unless otherwise specified) is the connection strength of coupling from CN1 to a PN, $w_{3,i}(t)$ is the modifiable connection strength of synaptic coupling from CN2 to the ith PN with saturation value $\tilde{w}_3 = 5$ (unless otherwise specified):

$$w_{3,i}(t) = \begin{cases} \tilde{w}_3, & T_{H,i} \leq t \leq T_{H,i} + \Delta h \\ 0, & \text{otherwise,} \end{cases} \tag{A.16}$$

$$\int_{T_{R,i}}^{T_{H,i}} \Theta(V_i(t) - \upsilon)\cdot\Theta(V_{N+2}(t) - \upsilon)\,dt = \frac{1}{\varepsilon}, \tag{A.17}$$

$$\Theta(x) = \begin{cases} 1, & x > 0 \\ 0, & x \leq 0, \end{cases} \tag{A.18}$$

where $T_{H,i}$ is the onset time when the plastic synaptic connection from CN2 to the ith PN becomes saturated, $T_{R,i}$ is the time of the previous reset of the plastic connection from CN2 to the ith PN,

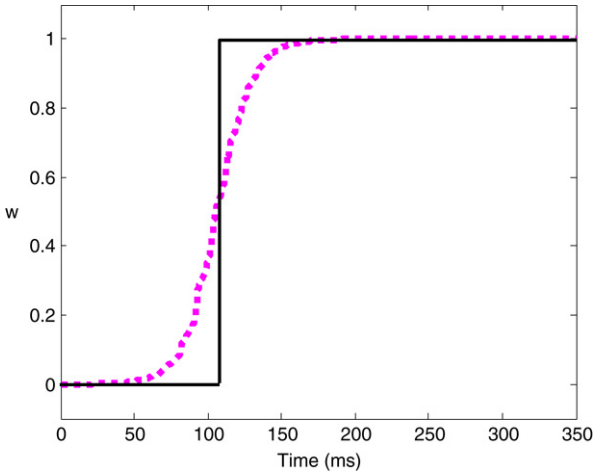

Fig. 9. The strength of coupling w versus time for the inhibitory connection from CN2 to PN. The dotted curve shows a sigmoidal increase of the connection strength induced by the coincidence of spikes from both neurons computed according to Eq. (B.1). In this equation parameters have the following values: $q_1 = q_2 = 0.01$, $c = 0.225$, $I_{ext} = 30$ mA for CN2 and $I_{ext} = 20$ mA for PN. The solid line shows the approximated step function which was employed in our simulations according to Eqs. (2.7) and (2.8).

i.e. the time when $w_3(t)$ last decayed to zero, $\Delta h = 650$ m s is the duration of short-term plasticity, $\upsilon = -10$ mV is the threshold value for synaptic plasticity, $\varepsilon = 0.16$ ms^{-1} is the learning rate.

Appendix B

The rule (2.8) for the modification of the GABAergic connection strength has been derived from the standard Hebbian type learning rule (Gerstner & Kistler, 2002). Let $w(t)$ be the coupling strength of the connection from CN2 to a PN. In a traditional form the dynamics of the connection strength can be written in the following way:

$$\frac{dw}{dt} = f(w)\,(1 + \tanh(q_1(V_{PN}(t) - \upsilon))) \times (1 + \tanh(q_2\,(V_{CN2}(t) - \upsilon))). \quad \text{(B.1)}$$

Here V_{PN} is the potential of PN, V_{CN2} is the potential of CN2. Learning is established when both neurons (CN2 and the PN) simultaneously generate action potentials ($V_{PN} > \upsilon$ and $V_{CN2} > \upsilon$, where υ is the threshold. The function for learning control $f(w) = c(w - w^2)$ provides saturation at the level $w = 1$. The parameter c is the rate of learning. To compare the dynamics of the connection strength modification, we simulated a model comprising the Hodgkin–Huxley equations for CN2 and PN together with Eqs. (2.8) and (B.1). The parameters in simulations were $\upsilon = -10$ mV, $\varepsilon = 0.16$/ms, $c = 0.225$, $q_1 = q_2 = 0.01$, $I_{ext} = 30$ mA for CN2 and $I_{ext} = 20$ mA for PN. The results presented in Fig. 9 show that our modification procedure is a step-wise approximation of the Hebbian learning rule.

References

Allman, L., Miezin, F., & McGuinness, E. (1985). Stimulus specific responses from beyond the classical receptive field: Neurophysiological mechanisms for local–global comparisons in visual neurons. *Annual Review of Neuroscience*, *8*, 407–430.

Andres, P. (2003). Frontal cortex as the central executive: Time to revise our view. *Cortex*, *39*, 871–895.

Baddeley, A. (1996). Exploring the central executive. *Quarterly Journal of Experimental Psychology*, *49A*, 5–28.

Baddeley, A. (2002). Fractionating the central executive. In D. Stuss, & R. T. Knight (Eds.), *Principles of frontal lobe function* (pp. 246–260). New York: Oxford University Press.

Barbas, H. (2000). Connections underlying the synthesis of cognition, memory, and emotion in primate prefrontal cortices. *Brain Research Bulletin*, *52*, 319–330.

Borisyuk, R., & Cooke, T. (2007). Metastable states, phase transitions, and persistent neural activity. *Biosystems*, *89*, 30–37.

Borisyuk, R., & Kazanovich, Y. (2004). Oscillatory model of attention-guided object selection and novelty detection. *Neural Networks*, *17*, 899–915.

Brager, D. H., Capogna, M., & Thompson, S. M. (2002). Short-term synaptic plasticity, simulation of nerve terminal dynamics, and the effects of protein kinase C activation in rat hippocampus. *Journal of Physiology*, *541*, 545–559.

Carlson, T. A., Hogendoom, H., & Ferstraten, F. (2006). The speed of visual attention: What time is it? *Journal of Vision*, *6*, 1406–1411.

Chelazzi, L., Miller, E. K., Duncan, J., & Desimone, R. (1993). A neural basis for visual search in inferior temporal cortex. *Nature*, *363*, 345–347.

Corbetta, M. (1998). Frontoparietal cortical networks for directing attention and the eye to visual locations: Identical, independent or overlapping neural systems. *Proceedings of the National Academy of Sciences of the United States of America*, *95*, 831–838.

Corchs, S., & Deco, G. (2001). A neurodynamical model for selective visual attention using oscillators. *Neural Networks*, *14*, 981–990.

Cowan, N. (1988). Evolving conceptions of memory storage, selective attention and their mutual constraints within the human information processing system. *Psychological Bulletin*, *104*, 163–191.

Damasio, A. (1989). The brain binds entities and events by multiregional activation from convergent zones. *Neural Computation*, *1*, 123–132.

Doesburg, S. M., Roggeveen, A. B., Kitajo, K., & Ward, L. M. (2008). Large-scale gamma-band phase synchronization and selective attention. *Cerebral Cortex*, *18*(2), 386–396.

Egeth, H. E., & Yantis, S. (1997). Visual attention: Control representation, and time course. *Annual Review of Psychology*, *48*, 269–297.

Fell, J., Fernandez, G., Klaver, P., Elger, C. E., & Fries, P. (2003). Is synchronized neuronal gamma activity relevant for selective attention? *Brain Research Reviews*, *42*, 265–272.

Fitzpatrick, J. S., Akopian, G., & Walsh, J. P. (2001). Short-term plasticity at inhibitory synapses in rat striatum and its effects on striatal output. *Journal of Neurophysiology*, *85*, 2088–2099.

Fries, P., Reynolds, J., Rorie, A., & Deimone, R. (2001). Modulation of oscillatory neuronal synchronization by selective visual attention. *Science*, *291*, 1560–1563.

Fries, P., Schroeder, J.-H., Roelfsema, P. R., Singer, W., & Engel, A. K. (2002). Oscillatory neural synchronization in primary visual cortex as a correlate of stimulus selection. *Journal of Neuroscience*, *22*, 3739–3754.

Gerstner, W., & Kistler, W. M. (2002). Hebbian models. In *Spiking Neuron Models: Single neurons, populations, plasticity*. Cambridge University Press (Chapter 10).

Gray, C. M. (1999). The temporal correlation hypothesis is still alive and well. *Neuron*, *24*, 31–47.

Herrmann, C. S., & Knight, R. T. (2001). Mechanisms of human attention: Event related potentials and oscillations. *Neuroscience and Biobehavioral Reviews*, *25*, 465–476.

Hodgkin, A. L., & Huxley, A. F. (1952). A quantitative description of membrane current and its applications to conduction and excitation in nerve. *Journal of Physiology*, *117*, 500–544.

Holscher, C. (2003). Time, space and hippocampal functions. *Review of Neuroscience*, *14*, 253–284.

Katayama, K., Yano, M., & Horiguchi, T. (2004). Neural network model of selective visual attention using Hodgkin–Huxley equation. *Biological Cybernetics*, *91*, 315–325.

Kazanovich, Y. B., & Borisyuk, R. M. (1994). Synchronization in a neural network of phase oscillators with the central element. *Biological Cybernetics*, *71*, 177–185.

Kazanovich, Y. B., & Borisyuk, R. M. (1999). Dynamics of neural networks with a central element. *Neural Networks*, *12*, 441–454.

Kazanovich, Y. B., & Borisyuk, R. M. (2003). Synchronization in oscillator systems with phase shifts. *Progress of Theoretical Physics*, *110*, 1047–1058.

Klein, R. (1988). Inhibitory tagging system facilitates visual search. *Nature*, *334*, 430–431.

Knight, R. T. (1997). Distributed cortical network for visual attention. *Journal of Cognitive Neuroscience*, *9*, 75–91.

Kryukov, V. I., Borisyuk, G. N., Borisyuk, R. M., Kirillov, A. B., & Kovalenko, E. I. (1990). Metastable and unstable states in the brain. In R. L. Dobrushin, V. I. Kryukov, & A. L. Toom (Eds.), *Stochastic cellular systems: Ergodicity, memory, morphogenesis* (pp. 225–358). Manchester University Press.

McAdams, C., & Maunsell, J. (1999). Effects of attention on orientation-tuning functions of single neurons of macaque cortical area V4. *Journal of Neuroscience*, *19*, 431–441.

Moran, J., & Desimone, R. (1985). Selective attention gates visual processing in the extrastriate cortex. *Science*, *229*, 782–784.

Morris, J. S., Friston, K. J., & Dolan, R. J. (1997). Neural responses to salient visual stimuli. *Proceedings of Royal Society, London B*, *264*, 769–775.

Niebur, E., & Koch, C. (1994). A model for the neuronal implementation of selective visual attention based on temporal correlation among neurons. *Journal of Computational Neuroscience*, *1*, 141–158.

Niebur, E., Hsiao, S. S., & Johnson, K. O. (2002). Synchrony: A neuronal mechanism for attention selection. *Current Opinion in Neurobiology*, *12*, 190–194.

Sillito, A. M., Grieve, K. L., Jones, H. E., Cudeiro, J., & Davis, J. (1995). Visual cortical mechanisms detecting focal orientation discontinuities. *Nature*, *378*, 492–496.

Singer, W. (1999). Neuronal synchrony: A versatile code for the definition of relations? *Neuron*, *24*, 49–65.

Steinmetz, P. N., Roy, A., Fitzgerald, P., Hsiao, S. S., Johnson, K. O., & Niebur, E. (2000). Attention modulates synchronized neuronal firing in primate somatosensory cortex. *Nature*, *404*, 187–190.

Takeda, Y., & Yagi, A. (2000). Inhibitory tagging in visual search can be found if search stimuli remain visible. *Perception and Psychophysics*, *62*, 927–934.

Tallon-Baudry, C., Bertrand, O., Henaff, M. A., Isnard, J., & Fischer, C. (2005). Attention modulates gamma-band oscillations differently in the human lateral occipital cortex and fusiform gyrus. *Cerebral Cortex*, *15*, 654–662.

Taylor, K., Mandon, S., Freiwald, W., & Kreiter, A. (2005). Coherent oscillatory activity in monkey area V4 predicts successful allocation of attention. *Cerebral Cortex*, *15*, 1424–1437.

Tiesinga, P. H. E. (2005). Stimulus competition by inhibitory interference. *Neural Computation*, *17*, 2421–2453.

Treisman, A., & Gelade, G. (1980). A feature-integration theory of attention. *Cognitive Psychology*, *12*, 97–136.

Vanduffel, W., Tootell, R., & Orban, G. (2000). Attention dependent suppression of metabolic activity in the early stages of the macaque visual system. *Cerebral Cortex*, *10*, 109–126.

Vidal, J. R., Chaumon, M., O'Regant, J. K., & Tallon-Baudry, C. (2006). Visual grouping and the focusing of attention induce gamma-band oscillations at different frequencies in human magnetoencephalogram signals. *Journal of Cognitive Neuroscience*, *18*, 1850–1862.

Vinogradova, O. S. (2001). Hippocampus as comparator: Role of the two input and two output systems of the hippocampus in selection and registration of information. *Hippocampus*, *11*, 578–598.

von der Malsburg, C. (2001). Neural basis of binding problem. In N. J. Smelser, & P. B. Baltes (Eds.), *International encyclopedia of social and behavioural sciences* (pp. 1178–1180). Elsevier.

Wang, D.-L., & Terman, D. (1995). Locally excitatory globally inhibitory oscillator network. *IEEE Transactions on Neural Networks*, *6*, 283–286.

Wang, D.-L., & Terman, D. (1997). Image segmentation based on oscillatory correlation. *Neural Computation*, *9*, 805–836.

Wang, D.-L. (1999). Object selection based on oscillatory correlation. *Neural Networks*, *12*, 579–592.

Zucker, R. S., & Regehr, W. G. (2002). Short-term synaptic plasticity. *Annual Review of Physiology*, *64*, 355–405.